Functional Materials 16, No.4 (2009)

Structure and magnetic state of films deposited by laser sputtering of nickel

A.G.Bagmut, I.G.Shipkova, V.A.Zhuchkov

National Technical University "Kharkiv Polytechnical Institute",
21 Frunze St. , 61002 Kharkiv, Ukraine

Received June 24, 2009

The influence of annealing on structure and phase states of nickel laser condensates has been studied. Volume changes, orientation relations between HCP and FCC crystal lattices, and magnetic properties changes after annealing are established. It has been shown that on (001) KCl substrate at a temperature higher than 400 K, a two-positioned nucleation and growth of HCP Ni grains takes place. Both positions contain groups of crystals with zone axes $[1\bar{1}1]$ and $[\bar{2}21]$ perpendicular to the substrate. The annealing of film initiates polymorphic HCP → FCC transformation accompanied by relative increasing of the material density by 18.5 %. The polymorphic transformation results in a change of the film magnetic characteristics: the film gets a magnetic moment, and hysteresis is observed at magnetic reversal.

Исследовано влияние отжига на структуру и фазовый состав лазерных конденсатов никеля. Выявлены объемные изменения и ориентационные соотношения между ГПУ и ГЦК решетками в пленках, а также изменение магнитных характеристик при отжиге. Показано, что на подложке (001) KCl выше 400 К имеет место двухпозиционное зарождение и рост зерен Ni со структурой ГПУ. Обе позиции содержат группы кристаллов, для которых оси зон $[1\bar{1}1]$ и $[\bar{2}21]$ ориентированы по нормали к подложке. Отжиг инициирует полиморфное превращение ГПУ → ГЦК, которое сопровождается относительным увеличением плотности вещества на 18.5 %. В результате полиморфного превращения происходит изменение магнитных характеристик пленки: пленки приобретают магнитный момент, а при перемагничивании наблюдается гистерезис.

At present, the pulse laser deposition (PLD) is used widely to produce films and coatings of various functional purposes [1]. The substance is deposited onto substrates as discrete portions from vapor-plasma flow which is formed at sputtering of a target by photon beam. The interest in Ni films and nanoparticles is caused by their magnetic, electric, and catalytic properties. At traditional thermal deposition of Ni onto (001) MgO surface, the nanostructures with hexagonal close-packed (hcp) lattice were observed [2]. When lateral sizes of granules exceed ~5 nm, the transformation from hcp to face-centered cubic (fcc) lattice occurs by martensite mechanism. The Ni nanoparticles of both hcp and fcc structures were obtained by deposition from solutions or by thermal decomposition of nickel organometallic precursors [3, 4]. Magnetic properties of Ni nanoparticles of hcp or fcc structures corresponded to both paramagnetic state and ferromagnetic one. Continuous Ni films of hcp or fcc structure were prepared by PLD methods [5, 6]. Only fcc Ni films revealed ferromagnetic properties.

The purposes of present work are to investigate the influence of thermal annealing on structure and phase composition of Ni laser films; to ascertain the volume changes and orientation relationships between hcp and fcc lattice in the films as well as the changes of magnetic properties at thermal annealing.

Table. Structure of thin laser Ni films

T_S (K)	290	350	420	520	660	700
Phase	Amorphous	α-Ni (hcp)	α-Ni (hcp)	α-Ni (hcp)	α-Ni (hcp)	β-Ni (fcc)

A high purity nickel target was sputtered by nanosecond pulses of an YAG:Nd^{3+} laser. At Q-switch mode and at pulse repetition frequency $\nu = 25$ Hz, the wavelength was 1.06 μm. The vapor-plasma Ni flux was deposited onto orienting substrates of KCl single crystals split along (001) cleavage planes. The films were separated from the substrate in distilled water and placed onto object grids for electron microscopic investigations. The substrate temperature was varied within the 290 K–700 K range. The residual gas pressure in vacuum chamber was about 10^{-5} Torr. Phase transformations in the films were initiated by two ways. In the first case, the post-deposition annealing in vacuum was applied to the samples without separation from the substrate. In the second one, the so-called "in situ" method was used. The film separated from substrate was heated in the microscope column using a special auxiliary device for sample heating. In this case, we had opportunity to observe continuously all stages of structure transformation.

The structure investigations were carried on using the electron diffraction method and the transmission electron microscopes PEM-100-01 and EM-100L. The film orientation with respect to substrate was determined using the angle between diffraction vector **g** in the microdiffraction pattern and the known substrate direction coinciding with the film edge image. The additional rotational displacement connected with the Lorentz rotation of the image relative to the diffraction pattern was compensated. The <100> KCl direction was used as the known direction of the substrate. This direction coincides automatically with the image of film edge when KCl substrate is split along {100} cleavage planes.

The magnetic characteristics of as-prepared Ni films and of those annealed at 670–700 K were investigated using a high-sensitive vibrating sample magnetometer. The hysteresis loops of the films were measured at room temperature using the square-shaped samples of 1 cm^2 area in magnetic fields up to 1000 Oe. The field was applied in the film plane in two mutually perpendicular directions. The mean saturation magnetization was determined by comparing the signals of the sample under study and the reference one characterized by known thickness and areas.

The following structure and phase states of thin films laser condensates were obtained at various substrate temperatures TS (Table): (i) Amorphous films; (ii) Ni films with metastable hcp lattice (α-Ni); (iii) Ni films of fcc structure (β-Ni).

In Fig. 1, the electron diffraction pattern and the TEM image of polycrystalline film deposited at $T_S = 350$ K are shown. The formation of the low-temperature (metastable) Ni phase of hcp structure was established by electron diffraction pattern identification and by comparing these results with data from crystallographic tables [7]. The mean grain size of α-Ni $<D>$ is 5.4 nm.

Elevation of T_S above 400 K causes an increased orientation extent of the films. The two-position generation and growth of α-Ni grains occur at the compliance with the following orientation relationships between the film and KCl substrate. At position 1:

$$(110)[\bar{1}1\bar{1}]\alpha\text{–Ni} \,//\, (110)[001]\text{KCl}, \quad (1a)$$

$$(110)[\bar{2}2\bar{1}]\alpha\text{–Ni} \,//\, (110)[001]\text{KCl}. \quad (1b)$$

The (1a) and (1b) relationships are observed for crystals belonging to $[\bar{1}1\bar{1}]$ and $[\bar{2}2\bar{1}]$ zone axes, respectively. In the first case, the $(\bar{5}59)$ plane of α-Ni is parallel to (001) surface of KCl substrate. In the second one, the (−10 10 9) plane of α-Ni is parallel to the above-mentioned surface.

At position 2:

$$(110)[\bar{1}1\bar{1}]\alpha\text{–Ni} \,//\, (\bar{1}10)[001]\text{KCl}, \quad (2a)$$

$$(110)[\bar{2}2\bar{1}]\alpha\text{–Ni} \,//\, (\bar{1}10)[001]\text{KCl}. \quad (2b)$$

The (2a) and (2b) relationships are realized for crystals belonging to $[\bar{1}1\bar{1}]$ and $[\bar{2}2\bar{1}]$ zone axes respectively. At $T_S \geq 700$ K, the epitaxial films are formed. Fig. 1c demonstrates the electron diffraction pattern and the TEM image of films deposited at $T_S =$ 700 K. Identification of electron diffraction pattern and comparison of the results with the data from crystallographic tables [8]

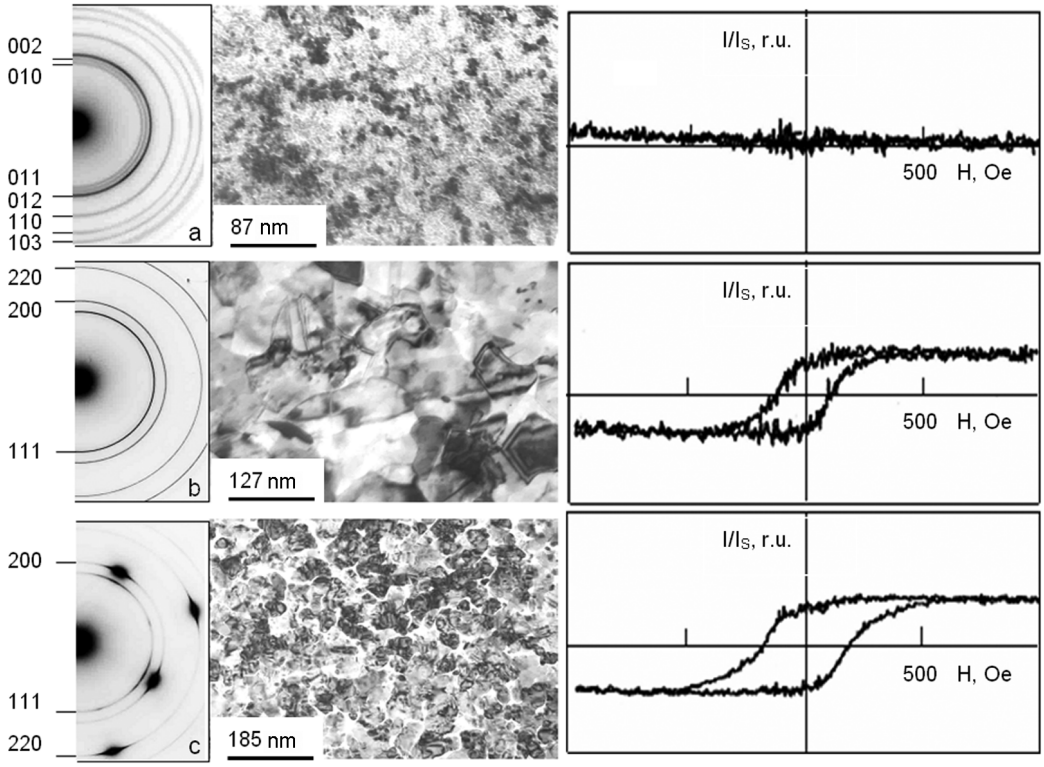

Fig. 1. Electron diffraction patterns, electron microscopy images and magnetization curves of films deposited from Ni laser erosion plasma; (a) hcp α-Ni film deposited at T_S = 350 K; (b) the same after annealing at 700 K during 120 min, the structure corresponds to fcc β-Ni phase; (c) epitaxial fcc β-Ni film deposited at T_S = 700 K.

have shown that in this case, the β-Ni high-temperature (stable) phase with fcc structure is formed. The mean grain size $<D>$ = 86.4 nm. The film grows in parallel orientation with respect to KCl substrate keeping within the simple orientation relationship:

$$(001)[110]\beta\text{–Ni} \,//\, (001)[110]\text{KCl} \qquad (3)$$

with the (001) surface of Ni film parallel to (001) one of KCl substrate.

It was found that the post-deposition annealing of films in vacuum initiates the phase transition when hcp lattice of Ni transforms to fcc lattice (Fig. 1b). The mean grain size $<D>$ increases from 5.4 nm to 87.8 nm. The annealing of "free" Ni films in the microscope column causes the hcp → fcc transformation, too. There is no noticeable changing of $<D>$ in this case. In Fig. 2 the result of "in situ" electron diffraction investigation of α-Ni (hcp) → β -Ni (fcc) polymorphic transformation under isothermal annealing (T_0 = 750 K, τ_0 = 40 min) in electron microscope column is shown. The initial α-Ni film was deposited at T_S = 420 K. In this case the partial ordering is observed and the orientation relationships hereinabove marked as (1) and (2) are kept. The diagram of electron diffraction pattern and its photo are shown in Fig. 2a and Fig. 2b, respectively. The reflections pertaining to α-Ni crystals with $[\bar{1}1\bar{1}]$ zone axis in position 1 are denoted by symbol "•". The reflections from α-Ni crystals with $[\bar{1}1\bar{1}]$ zone axis in position 2 rotated by 90° in the figure plane relative to position 1 are denoted as "■". The reflections from α-Ni crystals with $[\bar{2}2\bar{1}]$ zone axis in position 1 are denoted by "❍". Those from α-Ni crystals with $[\bar{2}2\bar{1}]$ zone axis in position 2 are denoted as "□. The identification of electron diffraction pattern of annealed film (Fig. 2c) has shown that β-Ni phase of fcc structure is formed.

According to Fig. 2, the diffraction vector $\mathbf{g} = 110$ of α-Ni crystals in position 1 with both $[\bar{1}1\bar{1}]$ and $[\bar{2}2\bar{1}]$ zone axes is parallel to diffraction vector $\mathbf{g} = 220$ of β-Ni crystals. Hence the following orientation relationships among the initial α-Ni phase and the final β-Ni one take place.

For position 1:

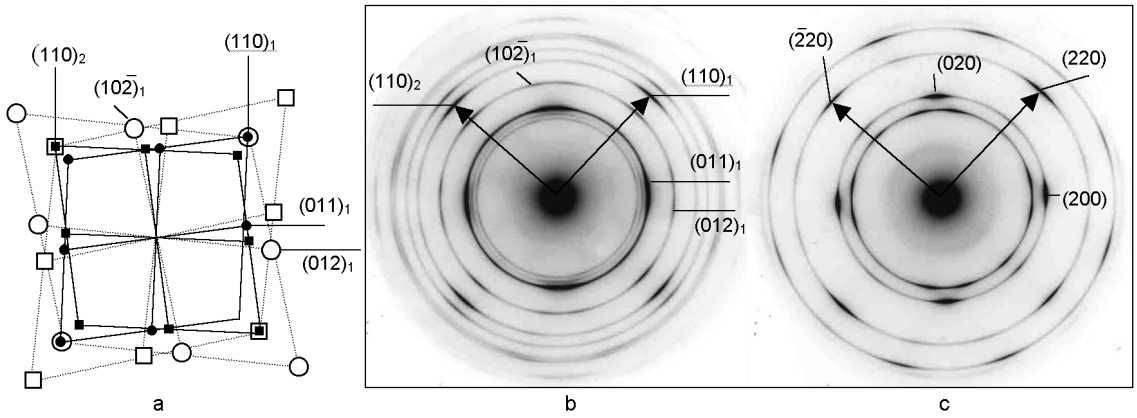

Fig. 2. *In situ* electron diffraction investigation of hcp → fcc polymorphous transformation at isothermal annealing of Ni film: (a), (b) Diagram and photo of electron diffraction pattern of Ni film before annealing (T_S = 420 K): reflections from • α-Ni crystals of [$\bar{1}1\bar{1}$] zone axis in position 1; ■ α-Ni crystals of [$\bar{1}1\bar{1}$] zone axis position 2; ❍ α-Ni crystals of [$\bar{1}1\bar{1}$] zone axis in position 1; □, α-Ni crystals of [$\bar{2}2\bar{1}$] zone axis in position 2. Electron diffraction pattern of the same films after annealing (T_a = 750 K, τ_a = 40 min).

$$(110)[\bar{1}1\bar{1}]\alpha\text{–Ni} \;//\; (110)[001]\beta\text{–Ni}, \qquad (4a)$$

$$(110)[\bar{2}2\bar{1}]\alpha\text{–Ni} \;//\; (110)[001]\beta\text{–Ni}. \qquad (4b)$$

The (4a) and (4b) relationships are observed for crystals in position 1 which belong to [$\bar{1}1\bar{1}$] and [$\bar{2}2\bar{1}$] zone axes, respectively.

For position 2:

$$(110)[\bar{1}1\bar{1}]\alpha\text{–Ni} \;//\; (\bar{1}10)[001]\beta\text{–Ni}, \qquad (5a)$$

$$(110)[\bar{2}2\bar{1}]\alpha\text{–Ni} \;//\; (\bar{1}10)[001]\beta\text{–Ni}. \qquad (5b)$$

The (5a) and (5b) relationships are correct for crystals in position 2 which belong to [$\bar{1}1\bar{1}$] and [$\bar{2}2\bar{1}$] zone axes, respectively.

When considering the histograms of grain size distribution for Ni films before and after annealing, it was found that in "free" films, the α-Ni → β-Ni polymorphic transformation is not accompanied by essential change of grain size. The mean grain size $\langle D \rangle$ is about 12 nm in both initial state and final one.

The relative change of Ni density γ being a result of phase transition from the state 1 with the density ρ_1 to the state 2 with the density ρ_2 was determined "in situ" in the microscope column according to [9]. The following relation was used:

$$\gamma = \frac{\rho_2 - \rho_1}{\rho_1} = \left(\frac{X_1}{X_2}\right)^3 - 1. \qquad (6)$$

In the relation (6), X_1 and X_2 are the distances between the same marks in Ni film at initial state (1) and final state (2), respectively. The film inhomogeneities, e.g., hardened Ni drops (so called "metal spray effect") have been used as the marks.

The phase transition from structure state of hcp-Ni lattice to fcc-Ni one was found to be accompanied by the film density increasing. Fig. 3 illustrates the change of Ni crystalline lattice under the film annealing in the microscope column using a special auxiliary device for sample heating. The α-Ni film was deposited at T_S = 350 K. The film structure (hcp structure prior to annealing) is shown in Fig. 3a. The annealing was carried out at T_a = 750 K during τ_a = 40 min. The film structure after annealing (fcc) is shown in Fig. 3b. The electron diffraction pattern and photomicrography were obtained after cooling of film down to room temperature in the microscope column.

It was established that in the case of hcp → fcc structure transition, the relative change of Ni density γ is 18.5±2.9 % (at confidence level 95 %). The density increase at hcp → fcc phase transition agrees with the data of the JCPDS tables. So according [7] and [8], the density of hcp Ni lattice ρ_1 = 7.372 g/cm^3 but that of fcc Ni lattice ρ_2 = 8.911 g/cm^3. According to the expression (6) γ = 20.9 %. This value is within the confidence interval of γ from 15.6 % to 21.4 % we have defined in our work.

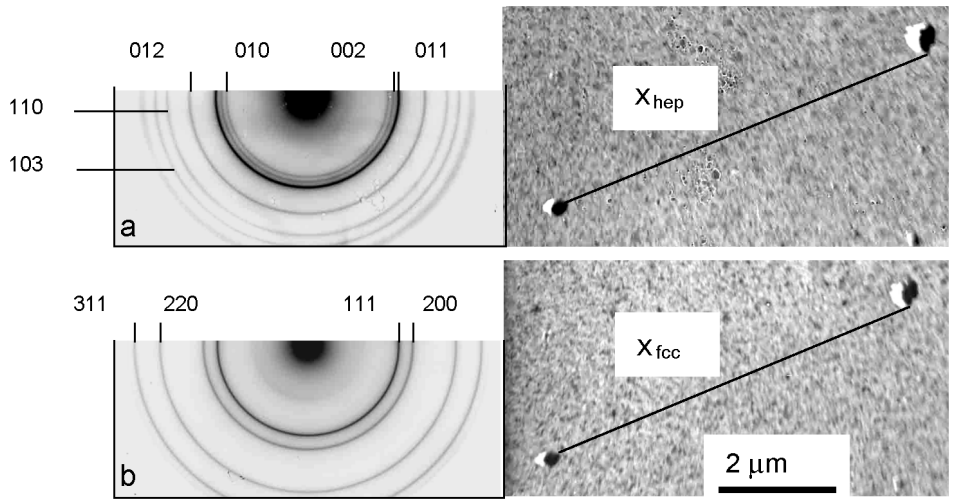

Fig. 3. Annealing of Ni film in electron microscope column: (a) Electron diffraction pattern and TEM image of film in as-prepared state (hcp lattice); (b) The same after annealing (fcc lattice).

The α-Ni films of metastable hcp structure do not reveal any magnetic moment exceeding the threshold of sensitivity of our magnetometer (see right-hand part of Fig. 1a). The magnetometer threshold of sensitivity corresponds to magnetization value less than 1–5 Gs at the sample geometric parameters mentioned above.

After annealing that initiates the hcp → fcc structure transformation, the magnetic state of films changes noticeably. Namely, the magnetic moment increases essentially and hysteresis is observed at magnetization reversal (see right-hand part of Fig. 1b). No anisotropy in the film plane is revealed. The coercive force H_C≈110 Oe, the saturation field H_S≈420 Oe. The similar magnetic characteristics for epitaxial ferromagnetic β-Ni film of fcc structure in as-prepared state after deposition at T_S = 700 K are as follows: H_C≈180 Oe, H_S≈700 Oe, saturation magnetization I_S = 320 Gs.

A variety of structure and phase states of laser Ni films we observed (see Table) is predefined by specific features of the PLD method. The main physical parameters of this method which define the structure formation are the density of vapor-plasma flux of sputtered metal; the flux density of gas particles present in the vacuum chamber; the tendency of metal to adsorb the gaseous impurities and to form chemical compounds therewith; the presence of ion component in deposited flux; the orientation and the temperature of substrate. At the same time, when laser sputtering of Ni target is used, the formation of non-crystalline thin solid structures is defined by the quenching of nonequilibrium states formed on the substrate immediately after deposition of each portion of substance and the chemisorption and implantation of gaseous impurities activated by high-energy ions of laser erosion plasma into the films. The last circumstance promotes the suppression of adatoms migration and of coalescence of noncrystalline complexes.

When T_S rises, the trapping of gaseous impurities by the growth surface decreases. Consequently, the migration of adatoms and the coalescence of noncrystalline complexes are intensified. This results in formation of crystalline films. The discreteness of substance arrival to substrate and small thickness of layer deposited during one deposition pulse initiate the action of phase dimensional factor. Formation of the metastable hcp α-Ni films should be interpreted in accordance with [10] as a phase transition connected with the decreasing film thickness. The transformation is conditioned by the change of free energy at increasing surface relative part.

The annealing at T_a = 700–750 K in vacuum of α-Ni films (both on substrate and in "free" state) initiates the recrystallization processes. In the film on substrate, the result of recrystallization is the increasing of Ni mean grain size <D> by one decimal order and the hcp → fcc transformation of the crystal lattice. The transformation in self-supported films occurs without essential change of <D>. The lower limit of the above temperature interval coincides with the epitaxial growth temperature of β-Ni

films at parallel orientation relative to (001) KCl substrate pre-specified by relation (3). The relation (3) is valid in the case of thermal evaporation and deposition on alkali halide crystal substrate, too.

Two positions of α-Ni films on (001) KCl substrate described by relations (1) and (2) are conditioned by equivalence of [110] and [1$\bar{1}$0] directions on the KCl substrate. These relations are similar to relations (4) and (5) that describe the orientation of α-Ni and β-Ni phases prior to and after film recrystallization, respectively. This is also connected with equivalence of [110] and [1$\bar{1}$0] directions of fcc β-Ni phase.

The change of the film magnetic moment observed in this work resulting from annealing may be explained by the change of Ni crystalline structure from metastable hcp (α-Ni phase) to equilibrium fcc structure (β-Ni phase). A model is known describing the electron structure of transition metal [11]. Within that model, the hcp Ni cannot possess any spontaneous magnetization whereas the fcc Ni is ferromagnetic. If that is the case, the change of magnetic properties after annealing are conditioned by magnetic phase transformation.

On the other hand, the contrary points of view exist. In [12], it is shown that hcp Ni is ferromagnetic with a magnetic moment of $0.59\mu_B$ being slightly smaller than that of the stable fcc Ni phase ($0.60\mu_B$). However, in nanodispersed thin film systems where the grains are isolated from each other and volume content of magnetic phase is less than 30 %, the superparamagnetism is possible. As a consequence, a low magnetic moment will be observed in magnetic fields below 1000 Oe.

The hcp α-Ni films deposited on (001) KCl are characterized by fine-grained polycrystal structure ($<D = 5.4$ nm) and by absence of magnetic moment. At the same time, the consideration of electron microphotos shown in Fig. 1a evidences a rather dense contact of grains. The transition to ferromagnetic state resulting from annealing of films on substrate is followed by increase of $<D>$ up to 87.8 nm. This is commensurable with grain sizes of as-prepared ferromagnetic films with $<D = 86.4$ nm. Those circumstances reinforce the assumption that the change in the film magnetic properties after annealing is conditioned by the magnetic phase transformation.

To conclude, when rising the substrate temperature ($T_S \geq 300$ K) at pulse laser deposition of nickel, the following structure and phase states of thin film laser films are formed sequentially: amorphous state, metastable hcp crystalline state (α-Ni phase), stable fcc crystalline state (β-Ni phase). The two-position nucleation and growth of α-Ni grains on (001) KCl substrate take place at $T_S \geq 400$ K. Both positions include the groups of crystals with axes of [$\bar{1}1\bar{1}$] and [$\bar{2}2\bar{1}$] zones oriented along the normal to substrate. The formation and growth of β-Ni film in parallel orientation relative to (001) KCl substrate occurs at $T_S \geq 700$ K. The annealing of metastable hcp Ni films initiates the polymorphous hcp → fcc transformation that occurs in accordance with orientation relationships (4) and (5) among phases and is accompanied by relative increasing of substance density by 18.5 %. As a result of α-Ni → β-Ni polymorphous transformation, the film magnetic characteristics are changed. The films get a magnetic moment, at magnetization reversal the hysteresis is observed.

References

1. Yu.K.Altudov, A.G.Garitsyn. Laser Microscale Technologies and Use Thereof in Electronics, Radio i Svyaz, Moscow (2001) [in Russian].
2. W.Tian, H.P.Sun, X.Q.Pan et al., *Appl. Phys. Lett.*, **86**, 131915-1 (2005).
3. Y.T.Jeon, J.Y.Moon, G.H.Lee et al., *J. Phys. Chem. B.*, **110**, 1187 (2006).
4. Y.Chen, D.-L.Peng, D.Lin, X.Luo, *Nanotechnolology*, **18**, 1 (2007).
5. A.G.Bagmut, I.G.Shipkova, V.A.Zhuchkov, *Functional Materials*, **16**, 1 (2009).
6. A.G.Bagmut, V.M.Kosevich, I.G.Shipkova et al., *Fizich. Ingeneria Poverkhn.*, **7**, 1 (2009).
7. International Center for Diffraction Data - JCPDC, 1996, card No.45-1027.
8. International Center for Diffraction Data - JCPDC, 1996, card No.04-0850.
9. USSR Authors Cert. No. 1689794 (publ. 1991).
10. A.I.Bublik, B.Ya.Pines, *Dokl. AN SSSR*, **87**, 215 (1952).
11. J.Goodinaf, Band Structure of Transition Metals and Alloys thereof, Izdat. Inostr. Liter., Moscow (1963) [in Russian].
12. X.He, L.T.Kong, B.X.Liu, *J. Appl. Phys.*, **97**, 106107 (2005).

Структура та магнітний стан плівок, осаджених лазерним розпилюванням нікелю

О.Г.Багмут, І.Г.Шипкова, В.А.Жучков

Досліджено вплив відпалу на структуру і фазовий склад лазерних конденсатів нікелю. Виявлено об'ємні зміни та орієнтаційні співвідношення між ГЩП та ГЦК гратками у плівках, а також зміни магнітних характеристик при відпалі. Показано, що на підкладці (001) KCl вище 400 К має місце двопозиційне зародження й ріст зерен Ni зі структурою ГЩП. Обидві позиції містять групи кристалів, для яких осі зон [111] і [$\bar{2}$21] орієнтовані за нормаллю до підкладки. Відпал ініціює поліморфне перетворення ГЩП $\rightarrow$ ГЦК, що супроводжується відносним збільшенням густини речовини на 18.5 %. У результаті поліморфного перетворення відбувається зміна магнітних характеристик плівки: плівки набувають магнітного моменту, а при перемагнічуванні спостерігається гістерезис.